Binding Partner Switching on Microtubules and Aurora-B in the Mitosis to Cytokinesis Transition*[S]

Nurhan Özlü‡§¶, Flavio Monigatti§‖, Bernhard Y. Renard§**, Christine M. Field‡, Hanno Steen§‖, Timothy J. Mitchison‡, and Judith J. Steen§‡‡§§

The cytoskeleton globally reorganizes between mitosis (M phase) and cytokinesis (C phase), which presumably requires extensive regulatory changes. To reveal these changes, we undertook a comparative proteomics analysis of cells tightly drug-synchronized in each phase. We identified 25 proteins that bind selectively to microtubules in C phase and identified several novel binding partners including nucleolar and spindle-associated protein. C phase-selective microtubule binding of many of these proteins depended on activity of Aurora kinases as assayed by treatment with the drug VX680. Aurora-B binding partners switched dramatically between M phase to C phase, and we identified several novel C phase-selective Aurora-B binding partners including PRC1, KIF4, and anaphase-promoting complex/cyclosome. Our approach can be extended to other cellular compartments and cell states, and our data provide the first broad biochemical framework for understanding C phase. Concretely, we report a central role for Aurora-B in regulating the C phase cytoskeleton. ***Molecular & Cellular Proteomics 9: 336–350, 2010.***

Cytokinesis requires coordinated reorganization of microtubules, actin, and membranes, which implies global regulation of cellular biochemistry. Animal cells are competent to undergo cytokinesis during a brief window in the cell cycle, called C phase, which starts shortly after cells exit mitosis (M phase) and lasts ~30–60 min (1, 2). The cytoplasm is globally regulated in M phase by the activity of one master kinase, Cyclin B-CDC2 (CDK1), that is strongly activated as cells enter M phase and controls the organization and function of 100s to 1000s of substrates (3, 4). C phase regulation, in contrast, is poorly understood. Given the global cytoplasmic changes that characterize C phase, global regulation by kinases seems likely. CDK1 activity decreases abruptly at anaphase onset, and the phosphatases that oppose it increase in activity (5). Thus, one global change in the transition from M to C phase is likely to be the loss of CDK1 phosphorylation, although the kinetics by which different substrates are dephosphorylated is unclear. Two other kinases, Aurora-B and PLK1, are broadly implicated in the regulation of C phase biochemistry and might function to some extent as global regulators (6). However, both these kinases are also active in M phase, and it is not clear how their activity and substrate specificities change between M and C phase.

Many cytoplasmic systems and compartments are likely to be controlled by C phase-regulating kinases. Here, we focus on the microtubule cytoskeleton as one specific compartment, although our methods could easily be adapted to any other compartment that could be isolated. Microtubules change dramatically in organization from the highly dynamic mitotic spindle in M phase to the less dynamic midzone and astral arrays in C phase. Several conserved proteins, including PRC1 and MKLP1, have been identified by cytology and genetics as C phase-specific microtubule-binding proteins that are required for midzone assembly and cytokinesis (7), but given the complexities of cytokinesis, others are likely to exist.

A major barrier to biochemical analysis of C phase in mammalian cells has been the lack of a method to synchronize cells in this phase. Synchronization in M phase with spindle-damaging drugs followed by washout allows only partial synchronization as C phase is short and cells take variable time to assemble spindles and exit M phase. Therefore, it is not possible to separate mitosis and C phase this way. We used a recently developed pharmacological approach; cells were arrested in monopolar mitosis where microtubule dynamics are relatively normal with a Kinesin-5 inhibitor and then forced into monopolar cytokinesis using a CDK1 inhibitor, giving excellent C phase synchrony (8, 9). This method works in part by global inhibition of CDK1, in part by activation of phosphatases (5), and in part by activating Cdh1 (through loss of inhibitory CDK1 phosphorylation (10)), which activates the anaphase-promoting complex/cyclosome (APC/C).[1] The net

From the ‡Department of Systems Biology, Harvard Medical School, Boston, Massachusetts 02115, §Proteomics Center at Children's Hospital Boston, Boston, Massachusetts 02115, Departments of ‡‡Neurobiology and ‖Pathology, Harvard Medical School and Children's Hospital Boston, Boston, Massachusetts 02115, and **Interdisciplinary Center for Scientific Computing, University of Heidelberg, D-069120 Heidelberg, Germany

Received, July 7, 2009, and in revised form, September 25, 2009
Published, MCP Papers in Press, September 28, 2009, DOI 10.1074/mcp.M900308-MCP200

[1] The abbreviations used are: APC/C, anaphase-promoting complex/cyclosome; NUSAP, nucleolar and spindle-associated protein; SILAC, stable isotope labeling by amino acids in cell culture; STC, *S*-trityl-L-cysteine; Pipes, 1,4-piperazinediethanesulfonic acid; NuMA, nuclear mitotic apparatus protein; INCENP, inner centromere protein; NPM1, nucleophosmin 1.

effect is to mimic most or all of the known regulation that occurs after normal anaphase onset. Cytological characterization of C phase induced in this way revealed that essentially all of the changes characteristic of C phase occur with relatively normal kinetics (11), so this method is a good starting point for investigating the biochemistry of cytokinesis.

We used LC-MS to characterize large scale changes in protein biochemistry in C phase. Although MS was previously used to identify midbody proteins (12), it has not been applied before to the problem of elucidating global C phase regulatory mechanisms. To allow quantitative comparison between phases, we used stable isotope labeling by amino acids in cell culture (SILAC) (13). Our approach can be likened to performing thousands of Western blots to compare microtubule- and Aurora-B-binding proteins between M phase, C phase, and interphase except that it was unbiased in terms of the proteins analyzed. Thus, our proteomic measurements provide a thorough evaluation of the biochemistry of each cell state as several measurements were made for each protein across two or three biological replicates, thus providing quantitative data with better accuracy than Western blots for thousands of proteins in multiple analyses (14). Furthermore, as we performed this analysis on a large scale, several known C phase proteins were identified and quantitated, thus generating several internal standards to validate the data. Using these approaches, we provide the first large scale description of C phase biochemistry and use chemical genetics to understand C phase.

MATERIALS AND METHODS

Cell Growth and Arrests

HeLa S3 cells were grown in Dulbecco's modified Eagle's medium (Caisson Laboratories) without lysine and arginine with 10% dialyzed fetal bovine serum (F0392; Sigma). Either light (^{12}C,^{14}N) or heavy (^{13}C,^{15}N) lysine and arginine amino acids (Sigma) were added in 0.146 and 0.08 4g/liter concentration, respectively. To arrest at mitosis, cells were first treated with 2 mM thymidine (Sigma) for 16 h; after 3 h of release, cells were treated with 10 μM *S*-trityl-L-cysteine (STC) for 12 h. For C phase, after 12 h of STC treatment, cells were treated with 100 μM purvalanol-A (Tocris Bioscience) for 15–20 min. Cells were washed extensively with PBS containing purvalanol-A and frozen. A double thymidine block protocol was followed for interphase synchronization. Subsequently, fluorescence-activated cell sorting (FACS) analysis and immunostaining were performed to confirm the cell stages.

Data Acquisition

Peptides derived from in-gel digested proteins were analyzed by on-line C_{18} nanoflow reversed phase HPLC (Eksigent nanoLC·2D^{TM}) hyphenated to a linear ion trap/orbitrap mass spectrometer (LTQ-Orbitrap, Thermo Scientific). Samples were loaded onto an in-house packed 100-μm-inner diameter × 15-cm C_{18} column (Magic C_{18}, 5 μm, 200 Å, Michrom Bioresources) and separated at 400 nl/min with 60-min linear gradients from 5 to 35% acetonitrile in 0.4% formic acid. Survey spectra were acquired on the Orbitrap with a resolution of 30,000. Up to six of the most intense ions per cycle were fragmented and analyzed in the linear trap.

The Thermo .raw files were converted into complete peak lists and entered into a relational database. The data conversion was performed using in-house written software utilizing the XRawfile2.dll library (version 2.1.1.0), which was provided by Thermo Scientific as part of the Xcalibur software package. The library is also used by MSQuant, Trans-Proteomic Pipeline, and the Sashimi project to convert the proprietary .raw file format into generic peak lists. For each MS/MS spectrum, the 200 most intense fragment ions were converted into an .mgf file without any further data processing such as smoothing, deisotoping, and filtering. Comparisons between the .mgf files generated by our approach and those generated by DTASuperCharge showed that our approach performed favorably.

Database Searches

Database searches were performed using Mascot (v.2.104) with 10–20-ppm precursor ion and 0.8-Da product ion search tolerances for MS2 data. Cysteine carbamidomethylation was used as a fixed modification, and pyroglutamic acid (N-terminal Gln), deamidation (Asn and Gln), oxidation (Met), and phosphorylation (Ser, Thr, and Tyr) were set as variable modifications. One missed tryptic cleavage was allowed.

Only the phosphopeptide hits with an ion score above the identity threshold as provided by the Mascot search were reported in this study with a false positive rate of 1%. For the phosphorylation analysis of non-labeled cells, ProteinPilot was used to analyze the data, and phosphopeptides with 95% and higher confidence were reported (15).

All peptides with a score above 33 were used for quantification for the microtubule binding assay and above 28 for Aurora-B immunoprecipitations. The data sets were searched against the International Protein Index human database (v.3.36) with 69,012 protein entries for the target database and 69,009 protein entries for the decoy database. A threshold of 33 resulted in an averaged false discovery rate of ~1%, and a score of 28 resulted in a false discovery rate of ~2%, estimated through the use of the decoy database searches. The SILAC ratios of all quantifiable peptides with good peaks were calculated using the MSQuant program (16). In microtubule pelleting assays and Aurora-B immunoprecipitations, phosphorylated peptides were excluded in the quantifications.

Microtubule Pelleting and Immunoprecipitation

M phase or interphase and C phase cells were lysed in a buffer (100 mM Pipes, 1 mM $MgCl_2$, 2 mM EGTA, 0.5% Nonidet P-40, 1 mM DTT) containing protease inhibitor (Roche Applied Science EDTA-free mixture tablet) and phosphatase inhibitors (1 μM okadaic acid, 1 μM microcystin, 10 mM NaF, 1 mM sodium orthovanadate, 1 mM β-glycerol phosphate, 1 mM sodium pyrophosphate). Lysates were precleared at 14,000 rpm for 5 min. Cell lysates were mixed in an equal concentration, determined using Bradford assay. The mixed supernatant was further clarified by centrifugation at 43,100 rpm (100,000 × *g*) in a TLA-100.3 rotor for 25 min at 4 °C. The supernatants were incubated either with 25 μM Taxol and 0.5 mM GTP for 20 min at room temperature or with Taxol-stabilized pure microtubules plus Taxol. Microtubules were pelleted through a 40% glycerol cushion in BRB80 (with protease inhibitors, phosphatase inhibitor, 1 mM DTT, 15 μM Taxol, 1 mM GTP) for 25 min at 43,000 rpm at 20 °C. The pellet was resuspended, loaded onto a second cushion, and spun as above (17). The pellet was resuspended in sample buffer and analyzed by SDS-PAGE. The Coomassie-stained gel was cut into 7–10 pieces; each gel piece was digested with trypsin (Promega).

For the microtubule pelleting experiment of VX680-treated C phase cells, cells were labeled either with the heavy or with the light isotope and arrested in mitosis as described above. One portion was treated

with purvalanol-A and 400 nM VX680 simultaneously, and the other was treated with purvalanol-A alone. Lysates were prepared and clarified. To deconvolute the role of Aurora-B in spindle assembly from its role in regulating the C phase cytoskeleton, Taxol-stabilized pure microtubules and Taxol were added to each lysate separately. The microtubules were then pelleted by centrifugation through glycerol cushions. Finally, the microtubule pellets were pooled in SDS sample buffer immediately before separation by SDS-PAGE. Because the microtubule pelleting experiments require more than 2 h to perform, we used this late pooling strategy to minimize the biochemical equilibration between the two samples, which would lead to an underestimation of the differences between the VX680 treatment and the control.

For Aurora-B immunoprecipitation, cells were lysed in 50 mM Hepes, pH 7.4, 150 mM KCl, 1 mM $MgCl_2$, 10% glycerol, 1 mM EGTA, 0.5% Nonidet P-40, 1 mM DTT including protease and phosphatase inhibitors as above. Lysates were pooled in an equal protein concentration following Bradford assays. The extract was incubated with protein A beads (Bio-Rad) alone followed by incubation with anti-Aurora-B antibody coupled with protein A to immunoprecipitate Aurora-B at 4 °C. Subsequently beads were washed extensively with lysis buffer, and the immunoprecipitates were eluted by boiling in 1× SDS sample buffer. The gel was cut into eight slices and in-gel trypsin-digested as described above.

Antibodies and Microscopy

For immunostaining or Western blotting, the following primary antibodies were used: Aurora-B (11) (AB3635; Abcam), FHOD-1 (18), PLK1 (raised against the C-terminal 15 amino acids), NuMA (sc18557), B23 (sc-32256), PRC1 (sc-8356), Cytokeratin-8 (sc-8020), CDC-27 (sc-9972; Santa Cruz Biotechnology, Inc.), α-tubulin (DM1A) (Sigma-Aldrich), KIF4 (A301-074A), MKLP2 (A300-879A; Bethyl Laboratories, Inc.), phospho-Histone H3 (06-570; Upstate), phosphomyosin light chain-2 (Ser-19) (3675; Cell Signaling Technology), and NUSAP (19). For immunoprecipitations, affinity-purified rabbit antibodies raised against the C-terminal 19 amino acids (C-WVRANSRRVLPPSALQSVA) of human Aurora-B were used. Imaging was done by a spinning disk confocal microscope (TE-2000; Nikon) controlled by the Metamorph imaging software (MDS Analytical Technologies).

Phosphoenrichment

The samples were separated using SDS-PAGE, the gel was cut into 10 slices, and each gel slice was trypsin-digested. TiO_2 was used to enrich for phosphopeptides. Briefly, lyophilized samples were dissolved in binding buffer (5% TFA, 40% acetonitrile). After loading samples onto the TiO_2 columns (TopTip, Glygen), the column was washed with the binding buffer. Phosphopeptides were eluted first with 100 mM ammonium bicarbonate and then with 0.4 M NH4OH, 40% acetonitrile.

Statistical Methodology

Transformation of Ratio Data—As the SILAC ratio data display an asymmetric grid with departures to the one side being exaggerated and to the other side being diminished, the data were transformed. Similar in its nature to the logarithmic transformation (20), we transformed a ratio value λ by $\lambda^o = \lambda/(\lambda + 1)$.

Peptide Level Analysis—For the phosphorylation analysis of total cell lysate, significance bounds were calculated using non-phosphorylated peptides from the flow-through of the phosphoenrichment analysis.

In the phosphorylation analysis of the microtubule binding assay, for the C phase selectivity, non-phosphorylated peptides of cytokinesis-selective microtubule-binding proteins were selected, whereas for the M phase selectivity, nonphosphorylated peptides of mitosis-selective microtubule-binding proteins were selected. For the non-phosphorylated peptides, we computed the respective transformed ratios for each repeat and then computed empirical confidence intervals for the ratios. For all phosphorylated peptides in the analysis, we identified those peptides showing significantly different ratios, outside the empirical confidence intervals (90%), over the various repeats.

When assuming no systematic departure of a peptide (so under the null hypothesis, H_0), the distribution of peptides within the interval is binomial. Considering the 90% confidence interval used, the probability of not being within this interval is $p = 0.1$. Thus, considering a peptide observed in n repeats and k times that is not within the interval, the p value for the departure from the majority of all peptides is given as p(minimum of k of the n observed peptides not in the interval) $= \Sigma_{m \geq k} \binom{n}{m} p^m (1 - p)^{n-m}$. Data from the phosphorylation analysis have been deposited in the Proteomics Identifications (PRIDE) database (57) with accession numbers 9971–9983.

Protein Level Analysis—To compare protein behavior against a reference protein, a peptide number-dependent approach was applied. For microtubule pelleting assays from different cell stages, the reference protein was tubulin. For microtubule pelleting with vs. without VX680 treatment, prepolymerized tubulin was added, so abundant housekeeper proteins, such as heat shock proteins and glyceraldehyde-3-phosphate dehydrogenase, were used as references. For the Aurora-B immunoprecipitation experiments, Aurora-B, tubulin, and actin were selected to have sufficient quantified reference peptides.

To discover whether a protein p_1 departed significantly from the reference protein p^r_1, the mean m_1 of the n transformed ratios of the peptides of p_1 was compared with a robust, nonparametric, bootstrap confidence interval for the mean of n peptides. Therefore, 1000 sets of n transformed peptide ratios were resampled with replacement from p^r_1, and for each of these sets, the mean was computed. Among these values, a 99% confidence interval was calculated. If the observed mean m_1 fell within this interval, it could not be concluded that p_1 departed from the reference protein.

Thus, for proteins with fewer quantified peptides, the confidence intervals are less stringent than for proteins with more quantified peptides. This allowed the elimination of proteins with fewer peptides unless they displayed a dramatic change between the two conditions.

RESULTS

Drug-based Synchronization in C Phase—Our synchronization methods are outlined in Fig. 1. HeLa S3 cells grown in suspension were arrested in monopolar mitosis using the Kinesin-5 inhibitor *S*-trityl-L-cysteine, and C phase was subsequently induced by adding the CDK1 inhibitor purvalanol-A for 15 min. Flow cytometry and microscopy data showed that synchronies of >90% were typically achieved for mitosis. Immunofluorescence was used to estimate C phase synchrony: cells in which phospho-Histone H3 staining was lost and microtubules were arranged in a monopolar midzone were scored as being in monopolar cytokinesis (11). By this criterion, >85% of the cells ($n = 64$) were in C phase following a 15-min treatment with purvalanol-A (Fig. 1). To determine whether C phase synchronization induced with a CDK1 inhibitor was a good biochemical surrogate for normal C phase, we collated a list of proteins known to be involved in C phase from the literature and interrogated our data to determine whether these proteins were C phase-selective under our

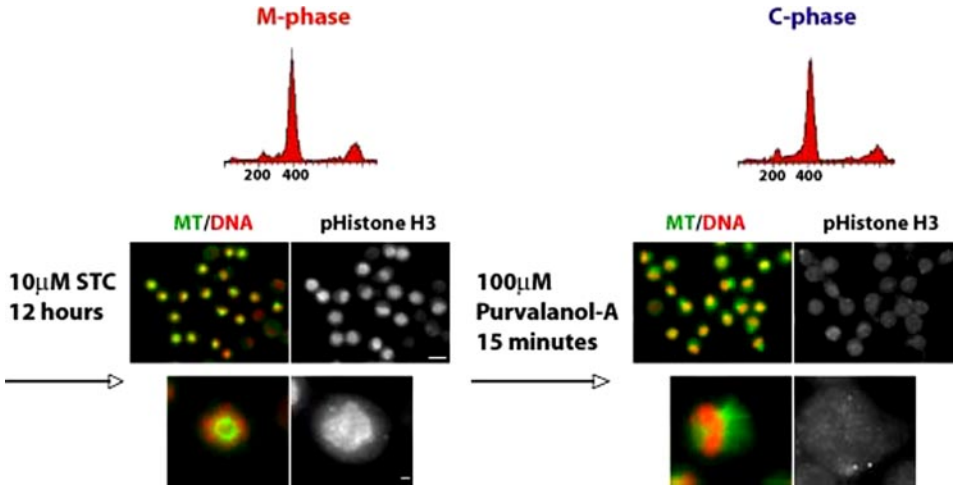

FIG. 1. **Drug-synchronized C phase HeLa S3 cells.** HeLa S3 cells were arrested in mitosis by treatment with 10 μM STC for 12 h, and subsequently C phase was induced by 100 μM purvalanol-A treatment for 15 min. The *top panel* shows the flow cytometry of M phase and C phase cells. M phase and C phase cells were stained for microtubules (*MT*) (*green*), DNA (*red*) and phospho-Histone (*pHistone*) H3. High magnification views of one cell from M phase and C phase are shown in the *bottom panel*. *Bars*, 10 μm (*upper*) and 1 μm (*lower*).

conditions (supplemental Table VI) within the experiments discussed below. We found an excellent correlation, suggesting that the drug synchronization method is valid for probing C phase biochemistry.

C Phase-selective Microtubule-binding Proteins—To identify C phase-selective microtubule-binding proteins, we combined clarified lysates from cells synchronized in C phase with either M phase or interphase lysates that were differentially labeled with heavy isotopes. We then polymerized endogenous tubulin with Taxol, sedimented the microtubules, and analyzed bound proteins (Fig. 2*A*). All the analyses in this study were performed on FTMS instruments. Fig. 2*B* shows a typical mass spectrum for a sample where C phase cells labeled with light lysine and arginine (Lys: $^{12}C_6$,$^{14}N_2$; Arg: $^{12}C_6$,$^{14}N_4$) were pooled with M phase cells labeled with heavy lysine and arginine (Lys: $^{13}C_6$,$^{15}N_2$; Arg: $^{13}C_6$,$^{15}N_4$). A false discovery rate calculation was performed for the peptides as described under "Materials and Methods." More than 1000 proteins were identified with two or more quantified peptides with Mascot scores of >33 (supplemental Table I). A significance value for the quantitative difference (ratio of M phase/C phase or C phase/interphase) for each protein was determined by comparison with tubulin as a reference protein (see "Materials and Methods"). Proteins that were marginally significant based on the bootstrap confidence interval were manually evaluated. Proteins that bound reproducibly to microtubules over three replicate experiments and that showed a statistically significant preference for binding in C phase or M phase lysates are shown in Table I. All microtubule-binding proteins observed and their isotope ratios are reported in supplemental Table I. To evaluate the reliability of our SILAC analysis, we used Western blotting and confirmed cell cycle selectivity of several putative M or C phase-selective microtubule binders (Fig. 2*C*).

Different groups of proteins showed different selectivity of microtubule binding in the three cell stages studied (Table I). Proteins enriched in C phase relative to both M phase and interphase include several known midzone-enriched proteins: KIF20A (also known as MLKP2) (21), RACGAP1 (22, 23), PRC1 (24, 25), and INCENP (26). The most striking novel C phase-selective binder is NUSAP. This is a potent microtubule-stabilizing and -bundling protein (27) and might be important for stabilizing the midzone. The fact that NUSAP is an importin substrate (19) and that the midzone protein TD60 is thought to have Ran guanine nucleotide exchange factor (GEF) activity (28) suggests the possibility that spatial regulation of the Ran system contributes to spatial organization of microtubules in C phase as it does in M phase (29). Another class of proteins that might contribute to C phase microtubule organization is the +tip proteins CLIP1, CLIP2, and CLASP1. Their M/C ratios were all ~0.3, implicating them in increasing microtubule stability as cells leave M phase. A novel C and interphase phase-selective binder was nucleophosmin (NPM1), a small, abundant phosphoprotein to which multiple functions have been ascribed (30). This protein was found in midbodies in a proteomics study (12) but had not otherwise been implicated in cytokinesis. Immunostaining showed NPM1 to be localized to the midbody late in cytokinesis (Fig. 2*D*). The C phase-selective subset also included several RNA processing enzymes whose significance is unknown. M phase-selective microtubule-binding proteins included several well known mitotic spindle proteins, including Kif22 (Kid), TACC3, and Aurora-A kinase. The most M phase-enriched was CKAP2L, a microtubule-associated protein that seems worthy of further study on the basis of this result.

M and C Phase-selective Protein Phosphorylation—Microtubule-binding proteins are often regulated by phosphorylation, and phosphorylation probably causes global cytoplas-

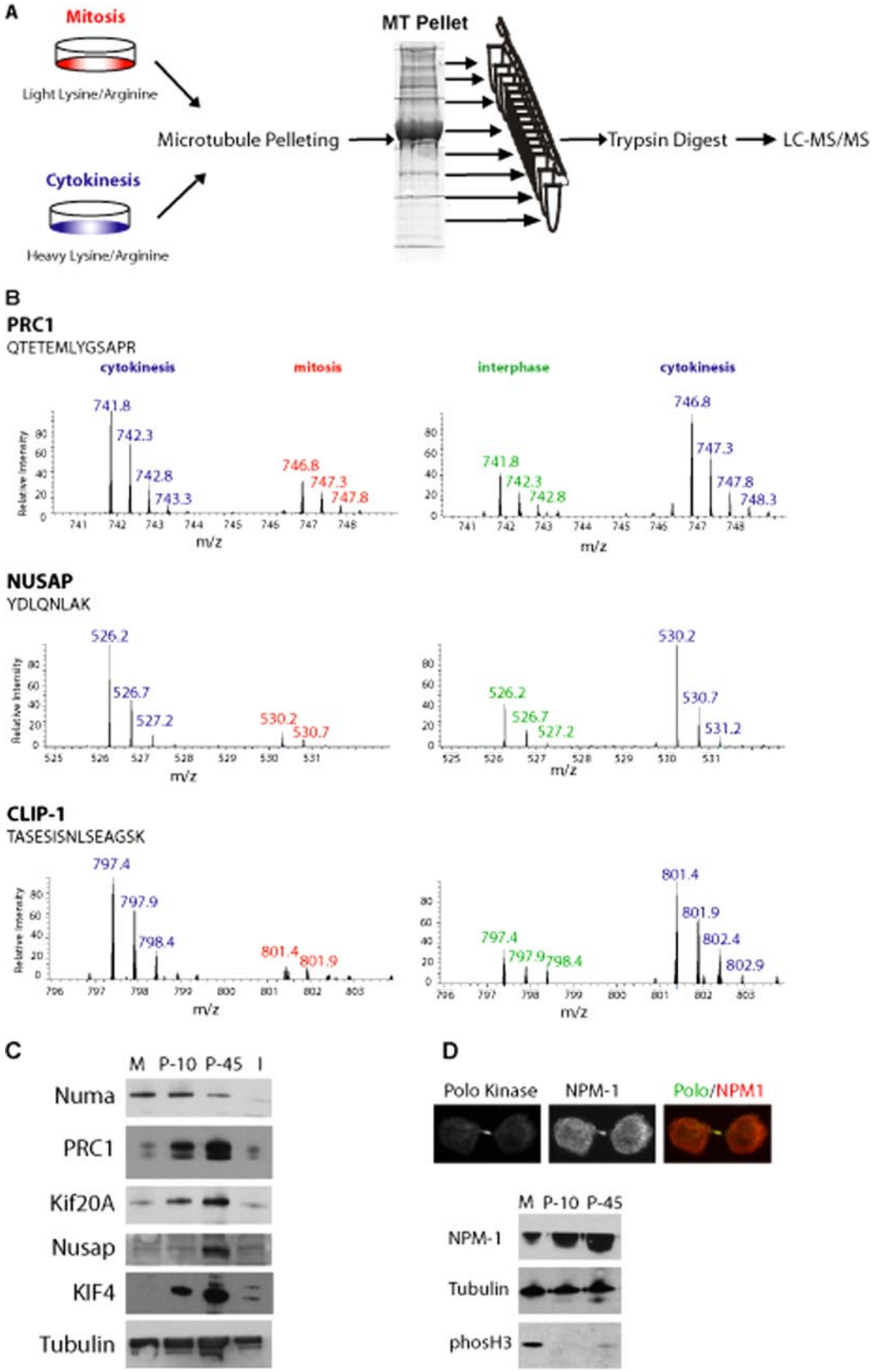

TABLE I
Microtubule pelleting assay using SILAC

Proteins that bind to microtubules preferentially in C phase or M phase are listed. M/C is the mean ratio of M phase (heavy) *versus* C phase (light) of quantified peptides; C/I is the mean ratio of C phase (heavy) *versus* interphase; STD is the standard deviation of the mean values; # Pep. represents the number of quantified peptides; U. # Pep. is the number of quantified unique peptides for M/C. The microtubule-binding proteins are grouped and color-coded by their SILAC ratios: yellow, M phase-selective; light yellow, both M and C phase-selective compared with interphase; blue, C phase-selective; light blue, C phase- and interphase-selective compared with M phase. The gray panel is the group of C phase-selective proteins that were not detected in C phase *versus* interphase experiments. MT, microtubule.

TUBB	0.8	0.1	0.8	0.2	tubulin	122	28
CKAP2L	3.4	1.8	2.9	0.5	cell cycle	7	6
KIF22	3.1	1.1	1.0	0.2	mitosis	7	5
CKAP2	2.3	0.7	2.7	0.8	cell cycle	11	8
TACC3	2.0	0.1			mitosis	3	1
AURKA	1.7	0.2	7.0	2.7	mitosis	41	16
KIF14	1.2	0.2	1.7	0.3	MT movement	92	48
KIF18A	1.2	0.2	2.5	0.4	MT movement	8	5
NUMA1	1.2	0.3	1.8	1.0	mitosis	118	87
CIT	1.1	0.5	2.1	0.6	mitosis, cytokinesis	74	44
HMMR	0.9	0.2	2.9	0.7	mitosis	60	35
PLK1	0.9	0.2	3.6	1.6	mitosis, cytokinesis	16	11
TPX2	0.8	0.3	4.6	1.3	mitosis	145	62
DLG7	0.8	0.3	3.5	0.7	mitosis	23	23
KIF23	0.8	0.1	4.0	1.4	cytokinesis	19	15
CENPE	0.8	0.6	3.0	1.8	mitosis	17	16
KIFC1	0.8	0.3	3.5	0.7	mitosis, cytokinesis	31	16
NUSAP1	0.2	0.1	2.6	0.6	cytokinesis, mitosis	47	28
TOP2A	0.3	0.3	1.8	0.2	DNA metabolism	14	8
NT5E	0.3	0.1	3.6	1.1	nucleotide catabolism	5	4
CLIP1	0.3	0.4	1.5	0.6	mitosis	46	29
KIF20A	0.4	0.0	3.8	2.2	cytokinesis	3	2
RACGAP1	0.5	0.5	3.7	0.1	cytokinesis	5	4
VIM	0.5	0.3	10.6	9.6	intermediate filament	39	16
RBM39	0.5	0.0	1.6	0.2	RNA processing	8	6
ELAVL1	0.4	0.1	1.7	0.6	RNA processing	9	7
ATP5A1	0.6	0.1	2.5	0.7	mitochondrial	32	13
INCENP	0.5	0.2	5.3	4.0	mitosis, cytokinesis	6	6
KIF2C	0.5	0.2	1.5	0.3	MT movement	3	3
FUSIP1	0.5	0.1	4.1		RNA processing	8	5
PRC1	0.6	0.1	3.1	0.6	cytokinesis	32	24
CEP170	0.2	0.1	1.2	0.1	centrosomal	17	11
KIF4A	0.3	0.1	1.1	0.3	cytokinesis	54	36
NPM1	0.3	0.1	0.8	0.5	RNA processing	80	18
EML3	0.4	0.2	0.6	0.1	MT organization	17	12
KIF2A	0.3	0.3	1.1	0.3	MT movement	10	8
TRIP12	0.3	0.1	0.6	0.0	ubiquitin cycle	2	2
DIDO1	0.5	0.1	0.6	0.1	apoptosis	11	7
CLTC	0.6	0.2	1.1	0.1	vesicle transport	75	39
MAP7	0.3	0.1	0.5	0.2	MT organization	21	15
MAP7D1	0.4	0.1	0.5	0.2	MT organization	12	7
SFPQ	0.5	0.1	0.7	0.2	RNA processing	9	6
SMN1	0.6	0.1	0.6	0.3	RNA processing	6	3
CLIP2	0.3	0.1			mitosis	7	5
CLASP1	0.4	0.2			mitosis	5	5
SPAG5	0.4	0.1			mitosis	6	5
ECT2	0.4	0.4			cytokinesis	3	2

mic changes during cell cycle progression. To identify proteins that are differentially phosphorylated between M and C phase, we performed phosphopeptide enrichment using TiO_2 on total lysate proteins. 50,000 MS2/MS3 spectra were acquired that identified ~4000 unique phosphopeptides in mitosis and ~3000 in cytokinesis (supplemental Table II). To obtain a more selective set of C phase-selective phosphorylation sites, phosphopeptide enrichment was combined with SILAC. Fig. 3*A* shows the distribution of all phosphopeptides from total clarified lysate in a typical SILAC comparison with M/C ratios displayed on a log scale (M was heavy in this experiment). Similar results were obtained in a biological replicate where the labels were switched (Fig. 3*A*). This curve is notably skewed to the M phase side, implying that there are more total phosphopeptides in M phase than C phase. A statistical analysis (see "Materials and Methods") revealed ~700 phosphorylation sites that were significantly enriched in M phase and ~170 in C phase (Fig. 3*B*). Table II summarizes some of the identified M phase- and C phase-selective phosphorylation sites (full data are in supplemental Table III). C phase-specific phosphorylations have been characterized for few proteins with the notable exception of intermediate filaments (31). We reidentified a C phase-specific Vimentin Ser-72 phosphorylation site (32) as a doubly phosphorylated Ser-71, Ser-72 peptide that was extremely C phase-specific (isotope ratio of 0.08 with M phase heavy (Table II)), validating our phosphopeptide analysis.

To more specifically probe the role of C phase phosphorylation in controlling microtubule organization, we analyzed phosphopeptides from microtubule-binding proteins by combining SILAC, microtubule isolation, and phosphopeptide enrichment. C phase selectivity in this experiment can arise either from selective binding of the protein to microtubules and/or C phase-selective phosphorylation. Most of the phosphorylation sites identified were common to both samples. 122 M phase and 72 C phase highly selective phosphorylation sites on microtubule-binding proteins were identified (Fig. 3*C* and supplemental Table III). This analysis confirmed several previously identified phosphorylation sites, including GLAP-NpTPGK (where pT is phosphothreonine) from PRC1 (a known CDK1 site (33)) and ASKSDATSGILNSpTNIQS from PRC1 (a known PLK1 site (34)). It also revealed many novel M

FIG. 2. **Relative quantification of microtubule-associated proteins in M phase, C phase, and interphase.** *A*, schematic of the microtubule (*MT*) pelleting assay using SILAC: lysates of C phase (labeled with light lysine and arginine) and M phase (labeled with heavy lysine and arginine) cells were pooled. Similarly, lysates of interphase (light) and C phase (heavy) cells were pooled. Microtubules were pelleted in the presence of Taxol by centrifugation. SDS-PAGE was used to separate total microtubule-binding proteins into fractions. Each gel slice was digested with trypsin, and the resulting peptide samples were analyzed using LC-MS/MS on a linear ion trap/orbitrap mass spectrometer (LTQ-Orbitrap). *B*, SILAC-based quantification of cell cycle-dependent PRC1- (*top*), NUSAP- (*middle*), CLIP1 (*bottom*)-microtubule interaction. The isotope ratios of C phase (light) *versus* M phase (heavy) and interphase (light) *versus* C phase (heavy) were quantified. Each protein is represented with a peptide. *C*, Western blotting analysis of microtubule pelleting samples from different cell cycle times: mitosis (*M*), C phase cells arrested in mitosis and treated with purvalanol for 10 min (*P-10*), C phase cells arrested in mitosis and treated with purvalanol for 45 min (*P-45*), and interphase (*I*). NuMA showed M phase-selective binding, whereas Kif20A, PRC1, and NUSAP showed C phase selectivity. *D*, immunostaining of a HeLa S3 cell probed for Polo kinase, NPM1, and the merge Polo (*green*)/NPM1 (*red*) (*top*). *Bar*, 5 μm. Western blotting of microtubule pelleting samples using NPM1, tubulin, and phospho-Histone H3 (*phosH3*) antibodies (*bottom*) is shown. Cell cycle abbreviations are as in *C*.

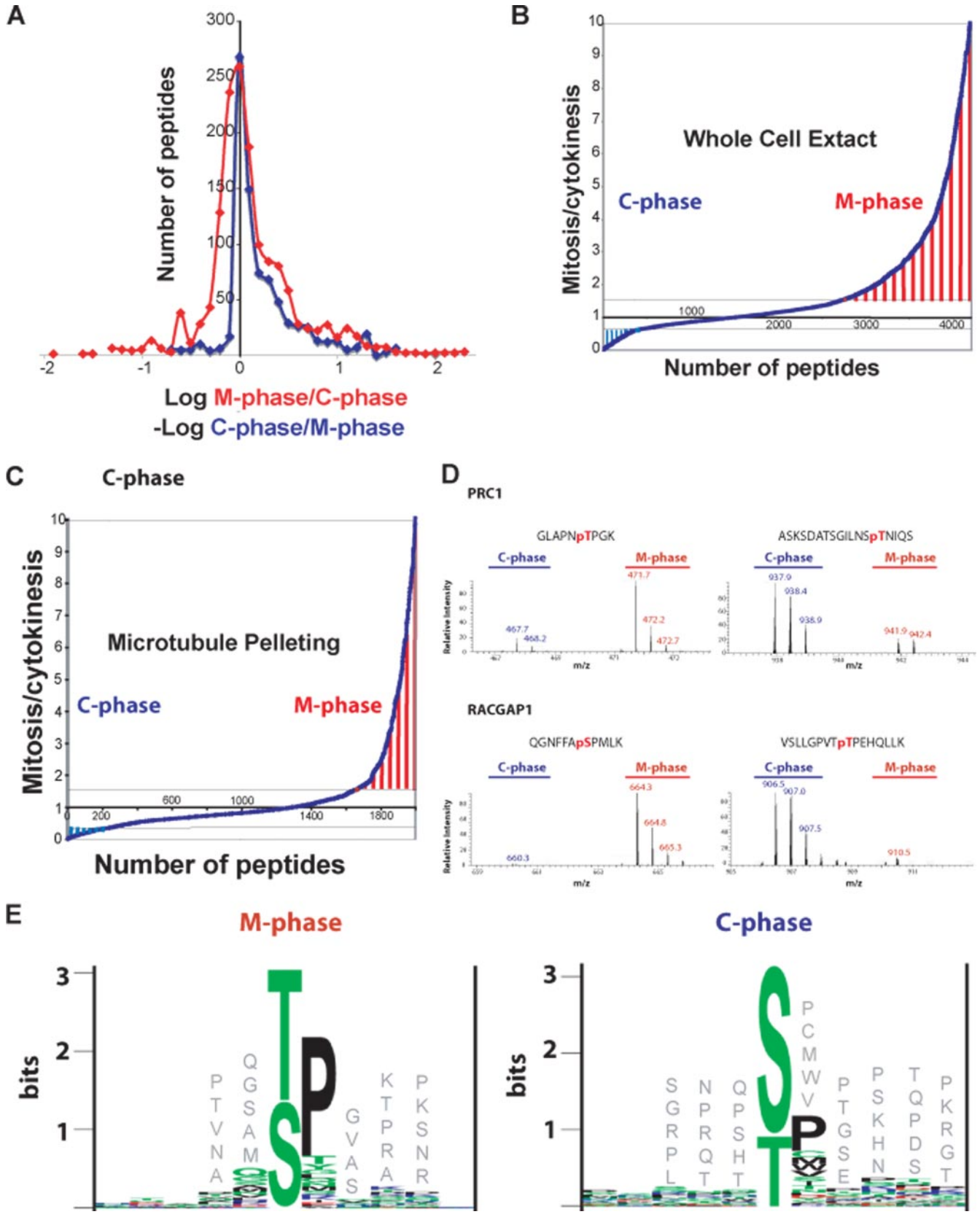

and C phase sites in microtubule-binding proteins (Fig. 3*D* and Table II). We used Sequence Logo (35, 36) to identify numerically dominant consensus phosphopeptide sequences for phosphopeptides from microtubule-binding proteins. In M phase, the dominant motif, (T/S)P*XX*(K/R) (Fig. 3*E*), was similar to the known CDK1 consensus motif. In C phase, (S/T)P still dominates, but it is not clear whether this is a CDK1 motif because the second position is less enriched in Pro and the fourth position shows less of a bias for basic residues. Interestingly, Aurora-B was the second notable consensus sequence listed. Further analyses showed that the Aurora kinase consensus sequences ((R/K)*X*(S/T)) was found in 14% of highly C phase-selective phosphopeptides ($n = 72$, M/C < 0.3) and 17% of moderately C phase-selective phosphopeptides ($n = 142$, M/C < 0.6), but only 7% of M phase selective phosphopeptides ($n = 123$, M/C > 1.6), suggesting that Aurora-B is an important regulator of C phase microtubule-associated proteins.

Aurora-B Kinase Broadly Regulates the C Phase Cytoskeleton—To dissect the role of Aurora-B kinase in regulating the C phase microtubule cytoskeleton, we took a chemical genetics approach using a small molecule kinase inhibitor. VX680 is a potent, selective inhibitor of Aurora kinases (37), and we previously showed that it blocked cell polarization and midzone assembly during monopolar cytokinesis (11). Here, we used SILAC to test how inhibiting Aurora kinases perturbed C phase microtubule-binding proteins. Microtubules were sedimented from VX680-treated and control C phase cells, and the samples were analyzed using mass spectrometry. Based on two biological replicates (heavy VX680/light mock or heavy mock/heavy VX680), we identified ~250 candidate microtubule-binding proteins that were perturbed by the VX680 treatment (supplemental Table IV). Fig. 4*A* shows a subset, focusing on annotated cytoskeleton proteins. Most cytoskeleton proteins were reduced in the microtubule pellet from VX680-treated cells, implying that phosphorylation by Aurora kinases *promotes* microtubule binding of many proteins in C phase, contrary to the general notion that phosphorylation tends to reduce microtubule binding affinity of microtubule-associated proteins (38). A notable exception was a group of kinetochore proteins (shaded *yellow*, together with NuMA) whose microtubule binding was increased by VX680. Aurora-B phosphorylation is known to decrease the affinity of the Ndc80 kinetochore complex for microtubules (39), suggesting that either other kinetochore proteins are similarly regulated or they tend to co-sediment with Ndc80.

VX680 treatment of C phase cells reduced the recovery of many known microtubule-binding proteins, including several we previously identified as C phase-selective in their binding in Table I (ECT2, KIF23 (MKLP1), KIF20 (MKLP2), RACGAP1, CLASP1, CLIP1, and Aurora-B itself). VX680 inhibits Aurora-A as well as Aurora-B, and some of its effects could be a result of Aurora-A inhibition, including microtubule binding of the known Aurora-A substrates TPX2 (40), TACC3 (41), DLG7 (42), HMMR (43), and Aurora-A itself (Fig. 4*A*). We also observed that myosin II and intermediate filaments (and some of their binding proteins) were reduced in the microtubule pellet from VX680-treated cells. Myosin II in particular was strongly perturbed; both its heavy and regulatory light chains were reduced in the pellet. It is not clear whether this important cleavage furrow motor is sedimenting by affinity to microtubules or actin filaments or because of its own polymerization, but it is clear that VX680 reduces its recruitment to the cytoskeleton, implying positive regulation of myosin II activity by Aurora kinases during cytokinesis. Co-sedimentation of intermediate filament proteins was also reduced by VX680 (Fig. 4*A*, shaded in *green*), suggesting that Aurora kinase activity is required in C phase for organization of all three parts of the cytoskeleton.

We retested the VX680 modulation of microtubule affinity of several proteins by Western blotting (Fig. 4*B*) and assayed inactivation of Aurora-B kinase activity in parallel using phospho-Histone H3 (Ser-10) (44). We found strong inhibition in both lysates and microtubule pellets. Phospho Myosin regulatory light chain (MRLC) (Ser(P)-19), which stimulates myosin II activity, was unaffected in lysates, demonstrating VX680 specificity, and reduced in the pellet, consistent with the MS results showing reduced recovery of myosin II protein in the pellet (Fig. 4*A*). Western blotting also confirmed several of our SILAC data points, such as Aurora-B itself and MKLP1.

Reduction of intermediate filament subunit recovery in the microtubule pellet by VX680 treatment was further analyzed to see whether it correlated with loss of phosphopeptides with likely Aurora-B consensus sequences. We performed a quantitative phosphopeptide enrichment with VX680 and mock-treated C phase cell extracts using SILAC as described above. Fig. 4*C* lists the Vimentin and Keratin-8 phosphorylation sites that are strongly diminished after VX680 treatment.

FIG. 3. **M phase and C phase phosphorylation analysis.** *A*, isotope ratio distribution of all phosphopeptides from clarified lysates. The *x axis* shows the M phase/C phase ratio on a log scale (*red*) and a replicate inverse isotope-labeled experiment in *blue*. Note that more phosphopeptides were recovered from mitotic lysates. *B*, number of M or C phase-selective phosphopeptides identified in clarified total lysate. This is the same data as in *A*, replotted to show the number of peptides for which the isotope ratio was significantly higher or lower than 1. The cutoff values for statistical significance are shown as *lines parallel* to the *x axis*. *C*, number of M or C phase-selective phosphopeptides identified in microtubule-binding proteins, plotted as in *B*. *D*, quantification of the known M phase-selective Thr-481 and C phase-selective Thr-602 phosphorylation sites on PRC1 (*top*) and the newly identified M phase-selective Ser-628 and C phase-selective Thr-580 phosphorylation sites on RACGAP1 (*bottom*) in M phase (heavy) *versus* C phase (light). *E*, the consensus motif of M phase phosphopeptides (*right*) and C phase phosphopeptides (*left*) from microtubule-binding proteins. Consensus was extracted using Sequence Logo.

TABLE II

Examples of M phase- and C phase-selective phosphorylation sites

#Pep represents the number of times a peptide was quantified in multiple experiments. Average (avg) Mascot scores are shown in the last column (see also supplemental Table III). Mean, standard deviation (st dev), median (med.), and median absolute deviation (mad) are calculated from the ratio M phase (heavy)/C phase (light). For each protein, C phase-selective phosphorylation sites are marked with C, and M phase-selective sites are marked with M. Bold residues in the sequence are phosphorylated: pS, phosphoserine; pT, phosphothreonine.

Protein	Sequence	Site	#Pep	M/C mean	st dev	M/C med.	mad	M/C	avg_score
PRC1	DPSLSD pSSpTVGLQR	T9	3	0.25	0.13	0.18	0.01	C	60
	ASKSDATSGILNS pTNIQS	T14	7	0.38	0.14	0.36	0.08	C	79
	NF pSIN pSVASTYSEFAK	S3,S6	7	0.44	0.23	0.36	0.07	C	64
	ENLELNG pS ILSGGYPGSAPLQR	S8	23	0.46	0.17	0.40	0.13	C	58
	QTETEMLYGSAPR pTPSK	T14	3	4.46	0.54	4.47	0.53	M	45
	GLAPN pTPGK	T6	10	7.40	3.02	6.60	2.30	M	36
CLASP1	NSSNT SVGpSPSNTIGR	S9	1	0.19		0.19		C	44
	RQ pSSGSATNVASTPDNR	S3	2	0.15	0.06	0.15	0.04	C	63
	SRpS DIDVNAAASAK	S3	2	0.39	0.06	0.39	0.04	C	57
CLASP2	VLVNSA pSAQKR	S7	2	2.93	0.47	2.93	0.33	M	53
CLIP1	KVQAEDEANGLQT pTPASR	T14	2	0.27	0.05	0.27	0.04	C	67
EB2	KpS HHAN pSPTAGAAK	S7	1	0.143		0.14		C	48
KIF4	GQVSESED pS ITK	S9	1	0.16		0.16		C	38
	NQ pSLVEENEK	S3	2	0.20	0.13	0.20	0.09	C	38
	FLEQ pSMDIEDLK	S5	9	0.28	0.10	0.28	0.07	C	58
	pT PPAPSPFDLPELK	T1	1	0.32		0.32		C	38
	QLEE pSVSEKEQQLLSTLK	S5	4	0.45	0.05	0.46	0.03	C	46
	QQGKD pS LGTVER	S6	3	0.50	0.06	0.47	0.01	C	38
	LTLLQVA pSR	S8	2	9.43	4.84	9.43	3.42	M	41
KIF14	DNR pTYVISASR	T5	1	0.27		0.27		C	40
CIT Kinase	SESVVSGLD pSPAK	S10	1	1.84		1.84		M	69
	VAS pSPAPPEGPSHPR	S4	3	3.80	0.52	3.72	0.40	M	53
NuSAP	pS LYTDESSKPGK	S1	2	0.17	0.02	0.17	0.01	C	45
	pS CGPASQ pSTLGLK	S1,S8	2	0.20	0.02	0.20	0.01	C	39
	VPpSPPDEHQEAENAVS pSGNR	S3,S17	13	0.26	0.12	0.23	0.09	C	59
	SAHVTVSGG pTPK	T10	9	11.40	9.16	7.85	2.46	M	59
	TITGNSAAVI pTPFK	T11	4	12.79	15.08	8.25	6.77	M	84
	LTTEATQ pTPVSNK	T8	3	13.89	2.87	14.08	2.59	M	51
DYNC1LI1	TGpSPGpSPGAGGVQSTAK	S3,S6	5	0.50	0.18	0.39	0.05	C	48
	QPPTAAGRPVDA pS PR	S13	2	2.54	0.21	2.54	0.15	M	45
INCENP	IAQV pSPGPR	S5	1	0.042		0.042		C	54
	VLAPILPDNFS pTPTGpS R	T12,S16	4	2.93	1.22	2.43	0.20	M	59
	YSLVAKQE pS VVR	S9	1	16.64		16.64		M	56
AURKB	KEPV pTPSALVLMSR	T5	1	14.28		14.28		M	42
RACGAP1	VSLLGPV pTpTPEHQLLK	T9	4	0.12	0.07	0.13	0.05	C	58
	TETDSVG pTPQSNGGMR	T8	4	11.31	9.71	9.33	5.58	M	48
	QGNFFA pSPMLK	S7	10	21.39	20.29	14.76	9.26	M	39
KIF23	AICGL pTPGRR	T6	2	25.54	12.23	25.54	8.65	M	31
KIF20A	EHSLQV pS PSLEK	S7	1	0.33		0.33		C	50
Anillin	TPIpSPLKTGVSKPIVK	S4	5	0.44	0.08	0.42	0.03	C	43
	AESGD pSLG pSEDRDLLYSIDAYR	S6,S9	4	3.50	0.81	3.37	0.61	M	48
Keratin-8	SYKV pS TSGPR	S5	6	0.24	0.07	0.25	0.03	C	46
	SYTSGPGSRIS pSpS pSFSR	S12,S13,S14	4	0.38	0.15	0.39	0.10	C	50
	VGpSSNFR	S3	8	2.40	0.71	2.26	0.33	M	48
	LESGMQNM pSIHTK	S9	4	3.87	0.03	3.87	0.03	M	47
	pSYpTSGPGSR	S1,T3	15	9.99	3.71	9.43	1.86	M	50
Keratin-7	SIHF pSpSPVFTSR	S5,S6	3	4.20	1.46	3.45	0.18	M	57
Keratin-17	TpSCRL pSGGLGAGSCR	S2,S6	4	3.76	0.66	3.72	0.37	M	48
Vimentin	LRp SpS VPGVR	S3,S4	8	0.08	0.08	0.06	0.04	C	38
	MFGGPGTA pSRP pSpS SR	S9,S12,S13	8	0.20	0.15	0.14	0.06	C	81
	LLEGEE pS RIpS LPLPNFSSLNLR	S7,S10	2	0.48	0.11	0.48	0.08	C	77
ZYX Zyxin	GPPAS pS PAPAPKFSPVTPK	S6	6	0.11	0.08	0.10	0.05	C	53
	FTPVA pSKF pSPGAPGGSGSQPNQK	S6,S9	7	0.32	0.09	0.29	0.06	C	47
NPM1	GPSpSVEDIK	S4	10	0.13	0.05	0.13	0.04	C	43
	DELHIVEAEAMNYEG pSPIK	S16	11	0.26	0.12	0.24	0.09	C	51
	SNQNGKD pSKP pSSTPR	S8,S11,T13	2	6.08	5.54	6.08	3.92	M	58
	MQA pSIEKAH	S4	32	10.32	5.69	8.51	2.87	M	54
	SIRD pTPAK	T5	1	29.29		29.29		M	29
KI-67	IACK pS PPPESVDTPTSTK	S4	2	0.04	0.00	0.04	0.00	C	51
	IACR pSPQPDPVGTPTIFKPQSK	S4	1	0.11		0.11		C	52
	IACK pS PQPDPVDTPASTK	S4	4	0.14	0.07	0.16	0.03	C	58
	AML pTPKPAGGDEKDIK	T4	1	2.22		2.22		M	49
	LTRT pSGEpT TQTHTEP pT GDSK	S5,T8,T16	5	3.55	0.35	3.72	0.18	M	52
	ASQPDLVD pTPTSSKPQPK	T9	2	8.72	0.40	8.72	0.28	M	53
	LDLTENL pTGSK	T8	2	26.92	14.50	26.92	10.25	M	64
	AFMG pTPVQK	T5	4	40.24	26.64	29.72	7.01	M	52

A

Protein Name	Mock / VX	STD	# Pep.	Group
ECT2	**4.7**	1.3	7	MT
CENPE	**3.1**	0.7	20	MT
TPX2	**2.7**	0.7	234	MT
AURKA	**2.6**	1.0	3	MT
DLG7	**2.6**	0.6	84	MT
TUBGCP3	**2.5**	0.5	39	MT
TUBGCP2	**2.5**	0.5	52	MT
RACGAP1	**2.3**	0.9	13	MT
CLIP1	**2.3**	0.7	32	MT
KIF23	**2.2**	0.5	95	MT
BICD2	**2.0**	0.5	27	MT
AURKB	**1.9**	0.4	13	MT
PCNT	**1.9**	0.4	47	MT
TACC3	**1.9**	0.2	7	MT
CLASP1	**1.8**	0.7	22	MT
KIF20A	**1.7**	0.3	74	MT
DCTN4	**1.7**	0.4	27	MT
PCM1	**1.6**	0.4	17	MT
HMMR	**1.6**	0.2	66	MT
CKAP5	**1.6**	0.3	82	MT
DYNC1LI2	**1.5**	0.3	45	MT
DYNC1H1	**1.5**	0.4	864	MT
KIF4	**1.5**	0.4	226	MT
NUSAP	**1.5**	0.2	86	MT
PRC1	**1.3**	0.4	91	MT
MYH10	**4.2**	1.2	11	actin
MYH11	**3.3**	1.0	16	actin
MYH9	**4.0**	1.3	134	actin
MYH14	**3.0**	1.0	10	actin
MRLC2	**3.2**	0.9	12	actin
Septin-10	**1.8**	0.3	10	actin
Septin-9	**1.7**	0.2	32	actin
MYO1C	**1.8**	0.4	9	actin
Septin-7	**1.8**	0.8	34	actin
ACTB	**1.7**	0.5	188	actin
Septin-6	**1.6**	0.3	21	actin
Septin-2	**1.6**	0.2	28	actin
ACTR1A	**1.7**	0.4	56	actin
ARHGEF2	**1.7**	1.1	55	actin
VIM	**6.4**	3.5	33	IMF
DES	**3.4**	0.8	4	IMF
Keratin-8	**3.2**	0.8	26	IMF
Keratin-18	**2.5**	0.5	16	IMF
NUMA1	**0.8**	0.3	273	MT
SPC24	**0.6**	0.5	8	Kinetochore
NSL1	**0.5**	0.4	3	Kinetochore
MIS12	**0.4**	0.1	2	Kinetochore
NUF2	**0.3**	0.1	3	Kinetochore
Spc25	**0.3**	0.1	3	Kinetochore

B

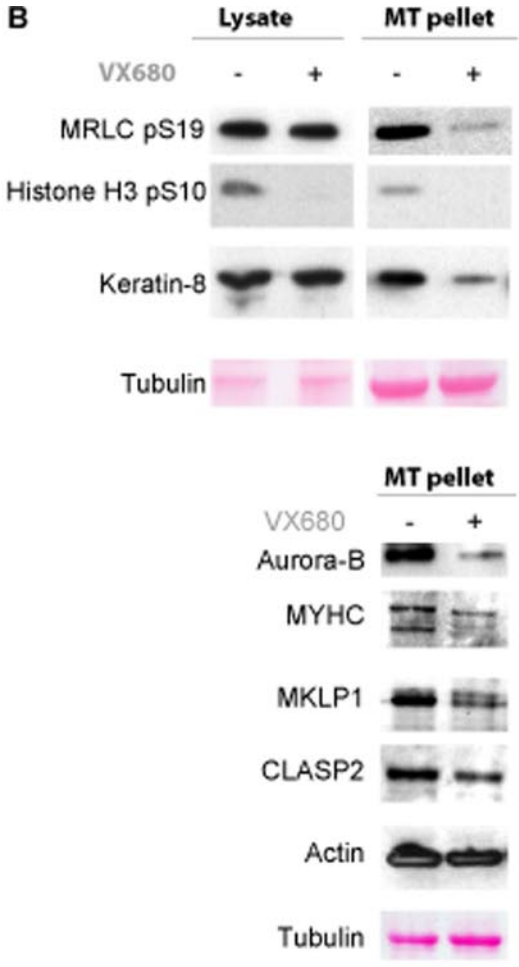

C

Protein Name	Sequence	Mock / VX680	STD	M/C	STD
Vimentin	LRpSpSVPGVR	12.50	1.33	0.08	0.08
	MFGGPGTApSRPpSpSSR	8.61	4.53	0.20	0.15
	SLYASpSPGGVYATRSpSAVR	10.00	8.02	3.82	3.52
Keratin-8	SYKVpSTSGPR	10.49	4.83	0.24	0.07
	SYTSGPGSRIpSSSpSFSR	8.45	1.43	0.38	0.15

D

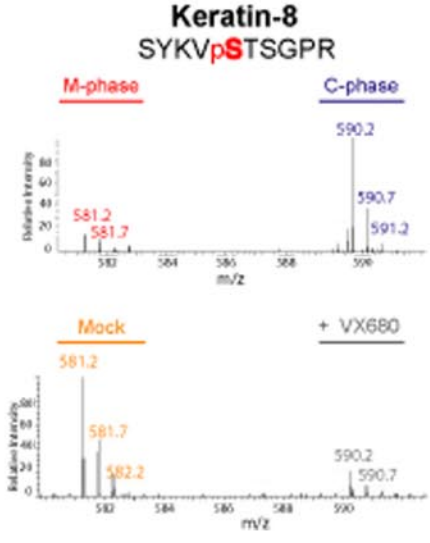

Most of these phosphorylation sites are C phase-selective. The Vimentin Ser-72 (LRpSSVPGVR where pS is phosphoserine) site was previously reported to be phosphorylated by Aurora-B in the cleavage furrow during normal cytokinesis (32). Fig. 4*D* shows the isotope ratios of the Keratin-8 Ser-13 (SYKVpSTSGPR) in M phase to C phase (*top*) and mock to VX680-treated C phase cell lysates (*bottom*). Keratin-8 Ser-13 phosphopeptide is clearly C phase-selective (5-fold elevated in C phase in comparison with M phase) and is affected by the VX680 treatment (10-fold diminished in VX680-treated C phase extracts; Fig. 4*D*), consistent with the hypothesis that Keratin, like Vimentin, is phosphorylated by Aurora-B during cytokinesis, perhaps to allow constriction of the cleavage furrow.

A Switch in Aurora-B Interactions between M Phase and C Phase—The data above show that Aurora kinases (most likely Aurora-B) play a central role in regulating the M to C phase switch in microtubule-binding proteins. However, we know that Aurora-B is active in both phases, so how can it mediate such a switch? One possibility is that the recruitment of the kinase to the vicinity of its substrates changes from M to C phase. To investigate how Aurora-B targeting changes between M and C phase, we characterized its binding partners, again using SILAC for quantitative comparisons. Differentially labeled lysates from M and C phase cells were pooled, and Aurora-B-binding proteins were isolated by immunoprecipitation. To decrease the influence of outliers possibly introduced by posttranslational modifications induced by Aurora-B kinase, we scored statistical significance from median and median absolute deviation values of the C/M ratio. These values were measured for three replicate experiments. We did not analyze interphase because Aurora-B is degraded at the end of C phase (45, 46). Fig. 5*A* shows a summary of proteins that selectively bind to Aurora-B in C phase or M phase. Full data are provided in supplemental Table V. Western blotting analysis was again used to confirm the SILAC data for selected proteins as shown in Fig. 5, *B* and *C*. A notable finding is that most of the C/M ratios are >1, and some are $\gg 1$. This indicates that Aurora-B gains many new binding partners as cells enter C phase. For several interactors, including PRC1, this change is essentially switchlike.

M phase-selective Aurora-B-binding proteins are shaded in *orange* in Fig. 5*A*. Aurora-B itself and other members of the Aurora-B complex (also known as the chromosomal passenger complex) display C/M ratios less than 1, indicating that less of the complex was recovered from the C phase lysate (see *asterisks*). This may reflect the onset of degradation of Aurora-B by the APC/C pathway (45). The C/M ratios of interacting proteins were not corrected for this loss of Aurora-B; thus, the C/M ratios in Fig. 5*A* under-report C phase selectivity of binding.

C phase-selective Aurora-B binders with known cell division roles are shaded in *blue* in Fig. 5*A*. Intriguingly, we found that several C phase-selective microtubule binders were also C phase-selective Aurora-B binders: PRC1, with a large C/M ratio, is essentially C phase-specific in its Aurora-B binding. PRC1 also binds selectively to microtubules in C phase (Table I) and may play a major role in targeting the kinase complex to midzone microtubules. Interestingly, the motor KIF4 is a strong interactor of Aurora-B during C phase. Because KIF4 also binds PRC1 (47), it is possible that a complex containing Aurora-B, PRC1, and KIF4 selectively assembles on C phase microtubules. SPAG-5/astrin also bound selectively to both microtubules and Aurora-B in C phase, and INCENP, a member of the Aurora-B complex, was also identified as a C phase-selective microtubule binder. The phosphosite analysis and these data together suggest two non-exclusive possibilities: the change in Aurora-B partners causes a change in Aurora-B localization, and the change in Aurora-B partners reveals a change in substrates of Aurora-B.

The formin FHOD-1 (48) was identified as a new interaction partner of Aurora-B in cytokinesis. A different formin, Diaphanous, is thought to nucleate cleavage furrow actin (49). FHOD-1 might contribute to the furrow or nucleate the actin cables observed to be associated with Aurora-B in and around the midzone during monopolar cytokinesis (11). We found that FHOD-1 localizes to the cortex in general but also to the midzone during cytokinesis where it colocalizes with Aurora-B (Fig. 5*D*). We also identified a phosphorylation site on FHOD-1 at Ser-367, RRpSL, an Aurora-B consensus sequence (supplemental Fig. S1). A prominent C phase-selective Aurora-B binder was the APC/C, several subunits of which appear in Fig. 5*A* (highlighted in *light orange*) with very high C/M ratios. Immunofluorescence showed that these two complexes overlap in localization at some stages of cytokinesis, for example in the midzone (Fig. 5*E*). Association between Aurora-B and CDC-27 was reported previously (45), but the association of the APC/C in the context of cytokinesis

FIG. 4. **Aurora-B kinase regulates C phase cytoskeleton.** *A*, the list of proteins that sediment with microtubules less efficiently in the presence of VX680: proteins shaded in *blue*, microtubule-related proteins (*MT*); *orange*, actin-related proteins; and *green*, intermediate filament-related proteins (*IMF*). Proteins that bind to microtubules more strongly in the presence of VX680 are shaded in *yellow*. The column headers are as follows: *Mock/VX*, the mean ratio of quantified peptides from mock- *versus* VX680-treated microtubule pellets; *STD*, S.D. values; # *Pep.*, the number of quantified peptides; *Group*, color codes the proteins according to Table I: *blue*, C phase-selective; *orange*, M phase-selective; *light gray*, no significant bias in M phase *versus* C phase; and *dark gray*, not detected. *B*, Western blotting of cell lysate and microtubule pellets of mock/VX680-treated cells against indicated proteins. The tubulin is from a Ponceau-stained membrane. *C*, list of phosphorylation sites of Vimentin and Keratin-8 proteins that are affected by the VX680 treatment. *D*, quantification of the phosphorylation site Ser-13 on Keratin-8 in M phase (light) *versus* C phase (heavy) and mock- (light) *versus* VX680 (heavy)-treated C phase cells.

A

Protein Name	C/M	MAD	Function	# Pep.	# U. Pep.
AURKB	0.6	0.1	bait	41	13
MKI67	0.6	0.1	DNA binding	4	3
H2AF.V, X, Y	0.5	0.0	DNA binding	4	4
RANGAP1	0.4	0.1	mitosis	5	5
INCENP*	0.3	0.2	mitosis, cytokinesis	66	24
CDCA8*	0.3	0.1	mitosis, cytokinesis	44	15
BIRC5*	0.3	0.1	mitosis, cytokinesis	11	6
PRC1	7.8	2.8	cytokinesis	11	9
PCM1	3.8	1.6	centrosomal organization	12	9
CEP170	2.7	0.9	centrosomal organization	8	4
FHOD1	1.5	0.2	actin cytoskeleton	33	19
KIF4A	1.4	0.3	cytokinesis	258	76
SPAG5	1.3	0.3	mitosis	79	31
VIM	1.2	0.2	cytoskeleton organization	16	12
KIF20A	1.0	0.5	cytokinesis	34	18
ANAPC1	11.1	1.4	cell cycle	3	3
CDC23	5.5	2.1	cell cycle	4	4
CDC27	5.1	0.5	cell cycle	7	7
ANAPC7	4.5	1.2	cell cycle	6	5
ANAPC5	3.3	0.1	cell cylce	2	2
SFRS7	4.2	0.7	RNA binding	5	2
RBM39	3.3	0.4	RNA binding	23	13
NPM1	2.7	1.2	RNA binding	5	5

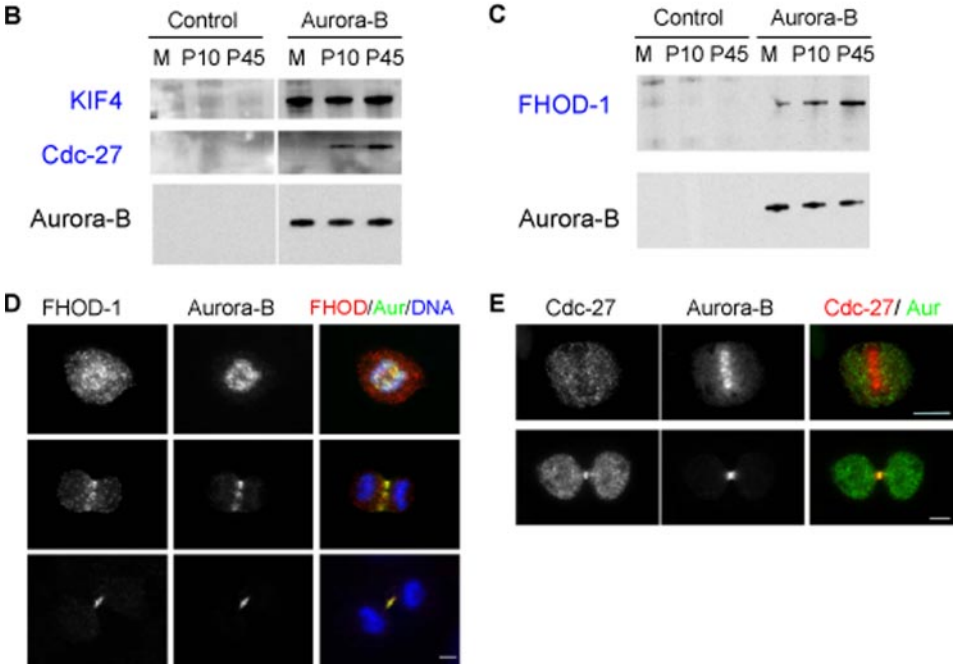

FIG. 5. **Switch in Aurora-B interactions in M phase and C phase.** *A*, major components of the M or C phase-selective Aurora-B co-immunoprecipitation are listed. The *orange* panel indicates the Aurora-B chromosomal passenger complex (indicated with *asterisks*) and/or M phase-selective interactors. The following three panels shaded in *blue* (cytoskeleton-related proteins), *light orange* (members of the APC/C), and *yellow* (proteins related to RNA metabolism) list proteins that were reproducibly enriched in C phase as compared with mitosis. The column headers are as follows: *C/M*, the C phase/M phase median ratios of all peptides quantified for the indicated protein; *MAD*, median absolute deviation; # *Pep.*, the number of quantified peptides; # *U. Pep.*, the number of quantified unique peptides. *B*, Western blotting of Aurora-B immunoprecipitation samples. Control IgG and Aurora-B elutants from M phase and C phase of purvalanol-A-treated for 10 min (*P10*) and purvalanol-A-treated for 45 min (*P45*) samples were probed with antibodies against KIF4, CDC-27, and Aurora-B. *C*, FHOD-1 and Aurora-B blotting of control and Aurora-B immunoprecipitants. Immunoprecipitation was performed for three different cell stages: mitosis (*M*), cytokinesis of purvalanol-A-treated for 10 min (*P10*), and purvalanol-A-treated for 45 min (*P45*). *D*, FHOD-1 and Aurora-B immunostaining of U2OS cells at anaphase (*top*), cytokinesis (*middle*), and late cytokinesis (*bottom*): FHOD-1, *red*; Aurora-B, *green*; DNA, *blue*. Aurora-B and FHOD-1 colocalize at the midzone microtubules. *Bar*, 5 μm. *E*, CDC-27 and Aurora-B immunostaining of HeLa cells at metaphase (*top*) and late cytokinesis (*bottom*): CDC-27, *red*; Aurora-B (*Aur*), *green*. CDC-27 localizes to the midbody. *Bars*, 5 μm.

and localization to the midzone is novel. We have confirmed this association by reciprocal immunoprecipitation (CDC-27 antibody in C phase lysate; data not shown).

DISCUSSION

The transition from M to C phase involves a major reorganization of microtubules and a significant change in their dynamics (50). They change again in the subsequent transition from C phase to interphase when loss of midzone proteins due to ubiquitination by CDH1/APC/C and proteolysis may be important (51). Our analysis of microtubule-binding proteins (Table I) showed that several mitotic spindle proteins lose affinity for microtubules as the cell enters C phase, and several known midzone and +tip proteins gain affinity. However, we observed much larger ratios for C phase-selective Aurora-B binding partners, suggesting that differential microtubule binding may be of a more graded nature, whereas Aurora-B partners change in a more switchlike manner.

Our analysis of protein phosphorylation in total clarified lysate and in microtubule-binding proteins revealed many more phosphopeptides that were M phase-selective than C phase-selective. This observation is consistent with two nonexclusive possibilities. (i) C phase is regulated by lack of CDK1 activity, and/or (ii) new phosphorylation sites are less important for C phase than for M phase. This possibility also emphasizes the dramatic activity of phosphatases during mitotic exit. Phosphopeptide analysis of microtubule-binding proteins nevertheless revealed many new sites in C phase, and ~17% of these had sequences consistent with their being Aurora-B substrates. Because several microtubule-binding proteins also interact with Aurora-B and VX680 inhibits its microtubule binding of several proteins, it is likely that some of these new C phase-selective sites are phosphorylated by Aurora-B. Overall, our data point to less global phosphorylation in C phase than M phase but suggest an important role for Aurora-B phosphorylation in positively regulating microtubule binding of many proteins, including several important midzone proteins. These data together with previous studies are illustrated in Fig. 6 (3–5, 7, 8).

Aurora-B is known to regulate various aspects of C phase, but the extent of its regulatory influence has been previously uncharted. This is the first time, to our knowledge, that chemical genetics and quantitative mass spectrometry have been used together to demonstrate the importance of kinase activities on mitotic exit and cytokinesis. Large scale proteomics analyses are crucial in revealing this broad effect of Aurora kinase activity. Blocking Aurora kinase activity with the potent inhibitor VX680 strongly reduced the microtubule binding efficiency of many microtubule-binding proteins. Only a small group of kinetochore proteins strongly gained affinity. The phosphorylation site analysis of C phase microtubule-binding proteins and the gain of Aurora-B interactors in C phase implicate Aurora-B as a central regulator of the microtubule organization in C phase. Association of activated myosin with

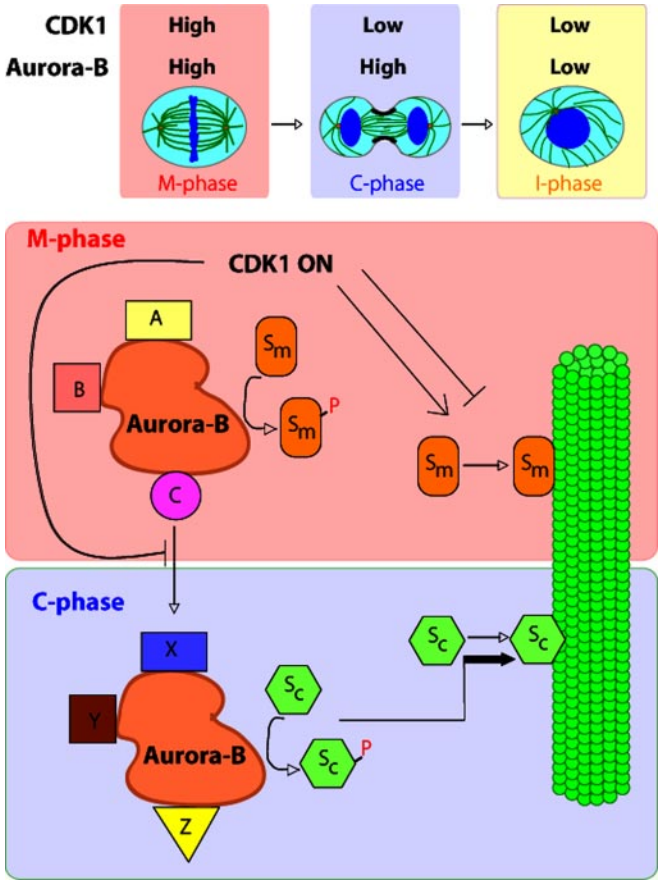

FIG. 6. **Schematic of CDK1 and Aurora-B kinases at different cell stages, illustrating changes in binding partners of Aurora-B kinase in M to C phase transition and its role in microtubule binding of C phase proteins.** *Sm* and *Sc* illustrate M and C phase substrates of Aurora-B, respectively. See the text for details. *I-phase*, interphase.

the cytoskeleton was also strongly reduced by VX680, suggesting that Aurora-B might directly regulate this central component of the contractile ring. The best characterized myosin regulatory phosphorylation, Ser-19 on the regulatory light chain, was not affected, suggesting that some other site(s) may govern myosin II regulation by Aurora-B. Intermediate filaments also undergo dramatic rearrangements during cytokinesis, and local phosphorylation in the cleavage furrow by Aurora-B was already implicated in rearrangement of Vimentin (32). Our data extend this idea to Keratin-8/18, which is a dominant intermediate filament class in dividing epithelial cancer cells (52, 53). Taken together, our data show that Aurora-B influences the intermediate filaments, microtubule, and actin cytoskeleton elements during C phase.

A challenge in understanding the role of Aurora-B is that the kinase itself is active in both M phase and C phase, so changes in its function are likely mediated by changes in interaction partners and/or subcellular localization. Dramatic spatial regulation of Aurora-B activity in cytokinesis was shown using fluorescence resonance energy transfer report-

ers for its activity (54). Our SILAC analysis of Aurora-B-interacting proteins reveals a similarly dramatic acquisition of new binding partners in C phase. In M phase, we mainly observed DNA-binding proteins binding to Aurora-B complex, whereas in C phase, microtubule-binding proteins and other cytoskeletal proteins were very prominent in the interaction list. C phase-selective Aurora-B binding partners include several proteins with known roles in cytokinesis as well as novel interactions, notably KIF4, APC/C, and FHOD-1. Overall, our data suggest that a switch in multiple Aurora-B partners is a major factor in regulating the biochemical transition from M to C phase.

The APC/C is known to play an important, but still poorly understood, role in cytokinesis (55), and proteosome-mediated proteolysis is thought to govern the orderly progression from mitosis through C phase to G_1 (51). We observed C phase-selective interaction between Aurora-B and APC/C, and both Aurora-B and CDC-27 localized to the midzone during the late cytokinesis stage. Consistent with these data, a recent study showed that CDH1/APC/C helps target Aurora-B kinase to the midzone (56). All these data support the idea that APC/C interactions with Aurora-B play a major regulatory role in C phase, perhaps especially in the midzone. We speculate that this interaction helps to target APC/C to relevant substrates as cytokinesis progresses, including the Aurora-B complex itself.

In summary, our analysis combines quantitative mass spectrometry with chemical genetics to provide the first broad overview of C phase biochemistry and reveals a large scale change of binding partners for microtubules and Aurora-B as cells enter C phase. It also provides evidence that Aurora-B should be considered one of the master regulatory kinases for C phase, at least for the microtubule cytoskeleton, because its activity is required to promote microtubule binding of many proteins during C phase. The mass spectrometry-based analyses described here provide a unique view of C phase that is complementary to using a single gene/protein perspective that is more traditionally used. Detailed analysis of any one of these interactions will yield more insights into local biochemistry, but proteomics methods are best suited to provide a global overview, and thus conceptual understanding, of how the cytoplasm is rearranged in the last step of the cell cycle.

Acknowledgments—We thank O. Fackler (University of Heidelberg, Heidelberg, Germany) for the antibody to FHOD-1, K. Ribbeck (Harvard University, Boston, MA) for the antibody to NUSAP, and N. Gray (Harvard University, Boston, MA) for Aurora-B inhibitor VX680. We thank M. Kirchner and W. Timm for input on the data analysis and storage, A. Guvenek and Z. Waldon for help with the sample preparation and data acquisition, and J. A. Vizcaino for help with PRIDE submission. We thank J. Paulo for critical reading of the manuscript.

* This work was supported, in whole or in part, by National Institutes of Health Grant GM 23928 (to T. J. M.). This work was also supported by a junior faculty development award from Children's Hospital Boston and Harvard Medical School (to J. J. S.).

S The on-line version of this article (available at http://www.mcponline.org) contains supplemental Fig. S1 and Tables I–VI.

¶ Supported by a long term postdoctoral fellowship from the European Molecular Biology Organization.

§§ To whom correspondence should be addressed: Division of Neuroscience, Children's Hospital Boston, 300 Longwood Ave., Boston, MA 02115. Tel.: 617-919-2450; Fax: 617-730-0168; E-mail: Judith.steen@childrens.harvard.edu.

REFERENCES

1. Rappaport, R. (1996) *Cytokinesis in Animal Cells*, Cambridge University Press, Cambridge, UK
2. Canman, J. C., Hoffman, D. B., and Salmon, E. D. (2000) The role of pre- and post-anaphase microtubules in the cytokinesis phase of the cell cycle. *Curr. Biol.* **10,** 611–614
3. Ubersax, J. A., Woodbury, E. L., Quang, P. N., Paraz, M., Blethrow, J. D., Shah, K., Shokat, K. M., and Morgan, D. O. (2003) Targets of the cyclin-dependent kinase Cdk1. *Nature* **425,** 859–864
4. Nurse, P. (1990) Universal control mechanism regulating onset of M-phase. *Nature* **344,** 503–508
5. Mochida, S., and Hunt, T. (2007) Calcineurin is required to release Xenopus egg extracts from meiotic M phase. *Nature* **449,** 336–340
6. Taylor, S., and Peters, J. M. (2008) Polo and Aurora kinases: lessons derived from chemical biology. *Curr. Opin. Cell Biol.* **20,** 77–84
7. Glotzer, M. (2005) The molecular requirements for cytokinesis. *Science* **307,** 1735–1739
8. Skoufias, D. A., Indorato, R. L., Lacroix, F., Panopoulos, A., and Margolis, R. L. (2007) Mitosis persists in the absence of Cdk1 activity when proteolysis or protein phosphatase activity is suppressed. *J. Cell Biol.* **179,** 671–685
9. Potapova, T. A., Daum, J. R., Pittman, B. D., Hudson, J. R., Jones, T. N., Satinover, D. L., Stukenberg, P. T., and Gorbsky, G. J. (2006) The reversibility of mitotic exit in vertebrate cells. *Nature* **440,** 954–958
10. Kramer, E. R., Scheuringer, N., Podtelejnikov, A. V., Mann, M., and Peters, J. M. (2000) Mitotic regulation of the APC activator proteins CDC20 and CDH1. *Mol. Biol. Cell* **11,** 1555–1569
11. Hu, C. K., Coughlin, M., Field, C. M., and Mitchison, T. J. (2008) Cell polarization during monopolar cytokinesis. *J. Cell Biol.* **181,** 195–202
12. Skop, A. R., Liu, H., Yates, J., 3rd, Meyer, B. J., and Heald, R. (2004) Dissection of the mammalian midbody proteome reveals conserved cytokinesis mechanisms. *Science* **305,** 61–66
13. Ong, S. E., Blagoev, B., Kratchmarova, I., Kristensen, D. B., Steen, H., Pandey, A., and Mann, M. (2002) Stable isotope labeling by amino acids in cell culture, SILAC, as a simple and accurate approach to expression proteomics. *Mol. Cell. Proteomics* **1,** 376–386
14. Mann, M. (2008) Can proteomics retire the western blot? *J. Proteome Res.* **7,** 3065
15. Shilov, I. V., Seymour, S. L., Patel, A. A., Loboda, A., Tang, W. H., Keating, S. P., Hunter, C. L., Nuwaysir, L. M., and Schaeffer, D. A. (2007) The Paragon Algorithm, a next generation search engine that uses sequence temperature values and feature probabilities to identify peptides from tandem mass spectra. *Mol. Cell. Proteomics* **6,** 1638–1655
16. Schulze, W. X., and Mann, M. (2004) A novel proteomic screen for peptide-protein interactions. *J. Biol. Chem.* **279,** 10756–10764
17. Budde, P. P., Desai, A., and Heald, R. (2006) Analysis of microtubule polymerization in vitro and during the cell cycle in Xenopus egg extracts. *Methods* **38,** 29–34
18. Gasteier, J. E., Madrid, R., Krautkrämer, E., Schröder, S., Muranyi, W., Benichou, S., and Fackler, O. T. (2003) Activation of the Rac-binding partner FHOD1 induces actin stress fibers via a ROCK-dependent mechanism. *J. Biol. Chem.* **278,** 38902–38912
19. Ribbeck, K., Groen, A. C., Santarella, R., Bohnsack, M. T., Raemaekers, T., Köcher, T., Gentzel, M., Görlich, D., Wilm, M., Carmeliet, G., Mitchison, T. J., Ellenberg, J., Hoenger, A., and Mattaj, I. W. (2006) NuSAP, a mitotic RanGTP target that stabilizes and cross-links microtubules. *Mol. Biol. Cell* **17,** 2646–2660
20. Graumann, J., Hubner, N. C., Kim, J. B., Ko, K., Moser, M., Kumar, C., Cox, J., Schöler, H., and Mann, M. (2008) Stable isotope labeling by amino acids in cell culture (SILAC) and proteome quantitation of mouse embryonic stem cells to a depth of 5,111 proteins. *Mol. Cell. Proteomics* **7,**

672–683
21. Hill, E., Clarke, M., and Barr, F. A. (2000) The Rab6-binding kinesin, Rab6-KIFL, is required for cytokinesis. *EMBO J.* **19,** 5711–5719
22. Mishima, M., Kaitna, S., and Glotzer, M. (2002) Central spindle assembly and cytokinesis require a kinesin-like protein/RhoGAP complex with microtubule bundling activity. *Dev. Cell* **2,** 41–54
23. Zhao, W. M., and Fang, G. (2005) MgcRacGAP controls the assembly of the contractile ring and the initiation of cytokinesis. *Proc. Natl. Acad. Sci. U.S.A.* **102,** 13158–13163
24. Mollinari, C., Kleman, J. P., Jiang, W., Schoehn, G., Hunter, T., and Margolis, R. L. (2002) PRC1 is a microtubule binding and bundling protein essential to maintain the mitotic spindle midzone. *J. Cell Biol.* **157,** 1175–1186
25. Jiang, W., Jimenez, G., Wells, N. J., Hope, T. J., Wahl, G. M., Hunter, T., and Fukunaga, R. (1998) PRC1: a human mitotic spindle-associated CDK substrate protein required for cytokinesis. *Mol. Cell* **2,** 877–885
26. Mackay, A. M., Ainsztein, A. M., Eckley, D. M., and Earnshaw, W. C. (1998) A dominant mutant of inner centromere protein (INCENP), a chromosomal protein, disrupts prometaphase congression and cytokinesis. *J. Cell Biol.* **140,** 991–1002
27. Raemaekers, T., Ribbeck, K., Beaudouin, J., Annaert, W., Van Camp, M., Stockmans, I., Smets, N., Bouillon, R., Ellenberg, J., and Carmeliet, G. (2003) NuSAP, a novel microtubule-associated protein involved in mitotic spindle organization. *J. Cell Biol.* **162,** 1017–1029
28. Mollinari, C., Reynaud, C., Martineau-Thuillier, S., Monier, S., Kieffer, S., Garin, J., Andreassen, P. R., Boulet, A., Goud, B., Kleman, J. P., and Margolis, R. L. (2003) The mammalian passenger protein TD-60 is an RCC1 family member with an essential role in prometaphase to metaphase progression. *Dev. Cell* **5,** 295–307
29. Caudron, M., Bunt, G., Bastiaens, P., and Karsenti, E. (2005) Spatial coordination of spindle assembly by chromosome-mediated signaling gradients. *Science* **309,** 1373–1376
30. Grisendi, S., Mecucci, C., Falini, B., and Pandolfi, P. P. (2006) Nucleophosmin and cancer. *Nat. Rev. Cancer* **6,** 493–505
31. Izawa, I., and Inagaki, M. (2006) Regulatory mechanisms and functions of intermediate filaments: a study using site- and phosphorylation state-specific antibodies. *Cancer Sci.* **97,** 167–174
32. Goto, H., Yasui, Y., Kawajiri, A., Nigg, E. A., Terada, Y., Tatsuka, M., Nagata, K., and Inagaki, M. (2003) Aurora-B regulates the cleavage furrow-specific vimentin phosphorylation in the cytokinetic process. *J. Biol. Chem.* **278,** 8526–8530
33. Zhu, C., Lau, E., Schwarzenbacher, R., Bossy-Wetzel, E., and Jiang, W. (2006) Spatiotemporal control of spindle midzone formation by PRC1 in human cells. *Proc. Natl. Acad. Sci. U.S.A.* **103,** 6196–6201
34. Neef, R., Gruneberg, U., Kopajtich, R., Li, X., Nigg, E. A., Sillje, H., and Barr, F. A. (2007) Choice of Plk1 docking partners during mitosis and cytokinesis is controlled by the activation state of Cdk1. *Nat. Cell Biol.* **9,** 436–444
35. Schneider, T. D., and Stephens, R. M. (1990) Sequence logos: a new way to display consensus sequences. *Nucleic Acids Res.* **18,** 6097–6100
36. Gorodkin, J., Heyer, L. J., Brunak, S., and Stormo, G. D. (1997) Displaying the information contents of structural RNA alignments: the structure logos. *Comput. Appl. Biosci.* **13,** 583–586
37. Harrington, E. A., Bebbington, D., Moore, J., Rasmussen, R. K., Ajose-Adeogun, A. O., Nakayama, T., Graham, J. A., Demur, C., Hercend, T., Diu-Hercend, A., Su, M., Golec, J. M., and Miller, K. M. (2004) VX-680, a potent and selective small-molecule inhibitor of the Aurora kinases, suppresses tumor growth in vivo. *Nat. Med.* **10,** 262–267
38. Andersen, S. S. (2000) Spindle assembly and the art of regulating microtubule dynamics by MAPs and Stathmin/Op18. *Trends Cell Biol.* **10,** 261–267
39. Cheeseman, I. M., Chappie, J. S., Wilson-Kubalek, E. M., and Desai, A. (2006) The conserved KMN network constitutes the core microtubule-binding site of the kinetochore. *Cell* **127,** 983–997
40. Bird, A. W., and Hyman, A. A. (2008) Building a spindle of the correct length in human cells requires the interaction between TPX2 and Aurora A. *J. Cell Biol.* **182,** 289–300
41. Giet, R., McLean, D., Descamps, S., Lee, M. J., Raff, J. W., Prigent, C., and Glover, D. M. (2002) Drosophila Aurora A kinase is required to localize D-TACC to centrosomes and to regulate astral microtubules. *J. Cell Biol.* **156,** 437–451
42. Wong, J., Lerrigo, R., Jang, C. Y., and Fang, G. (2008) Aurora A regulates the activity of HURP by controlling the accessibility of its microtubule-binding domain. *Mol. Biol. Cell* **19,** 2083–2091
43. Groen, A. C., Cameron, L. A., Coughlin, M., Miyamoto, D. T., Mitchison, T. J., and Ohi, R. (2004) XRHAMM functions in ran-dependent microtubule nucleation and pole formation during anastral spindle assembly. *Curr. Biol.* **14,** 1801–1811
44. Hirota, T., Lipp, J. J., Toh, B. H., and Peters, J. M. (2005) Histone H3 serine 10 phosphorylation by Aurora B causes HP1 dissociation from heterochromatin. *Nature* **438,** 1176–1180
45. Nguyen, H. G., Chinnappan, D., Urano, T., and Ravid, K. (2005) Mechanism of Aurora-B degradation and its dependency on intact KEN and A-boxes: identification of an aneuploidy-promoting property. *Mol. Cell. Biol.* **25,** 4977–4992
46. Honda, K., Mihara, H., Kato, Y., Yamaguchi, A., Tanaka, H., Yasuda, H., Furukawa, K., and Urano, T. (2000) Degradation of human Aurora2 protein kinase by the anaphase-promoting complex-ubiquitin-proteasome pathway. *Oncogene* **19,** 2812–2819
47. Zhu, C., and Jiang, W. (2005) Cell cycle-dependent translocation of PRC1 on the spindle by Kif4 is essential for midzone formation and cytokinesis. *Proc. Natl. Acad. Sci. U.S.A.* **102,** 343–348
48. Schönichen, A., Alexander, M., Gasteier, J. E., Cuesta, F. E., Fackler, O. T., and Geyer, M. (2006) Biochemical characterization of the diaphanous autoregulatory interaction in the formin homology protein FHOD1. *J. Biol. Chem.* **281,** 5084–5093
49. Goode, B. L., and Eck, M. J. (2007) Mechanism and function of formins in the control of actin assembly. *Annu. Rev. Biochem.* **76,** 593–627
50. Eggert, U. S., Mitchison, T. J., and Field, C. M. (2006) Animal cytokinesis: from parts list to mechanisms. *Annu. Rev. Biochem.* **75,** 543–566
51. Lindon, C., and Pines, J. (2004) Ordered proteolysis in anaphase inactivates Plk1 to contribute to proper mitotic exit in human cells. *J. Cell Biol.* **164,** 233–241
52. Fuchs, E., and Cleveland, D. W. (1998) A structural scaffolding of intermediate filaments in health and disease. *Science* **279,** 514–519
53. Chu, P. G., and Weiss, L. M. (2002) Keratin expression in human tissues and neoplasms. *Histopathology* **40,** 403–439
54. Fuller, B. G., Lampson, M. A., Foley, E. A., Rosasco-Nitcher, S., Le, K. V., Tobelmann, P., Brautigan, D. L., Stukenberg, P. T., and Kapoor, T. M. (2008) Midzone activation of aurora B in anaphase produces an intracellular phosphorylation gradient. *Nature* **453,** 1132–1136
55. Chew, T. G., and Balasubramanian, M. K. (2008) Nuc2p, a subunit of the anaphase-promoting complex, inhibits septation initiation network following cytokinesis in fission yeast. *PLoS Genet.* **4,** e17
56. Floyd, S., Pines, J., and Lindon, C. (2008) APC/C Cdh1 targets aurora kinase to control reorganization of the mitotic spindle at anaphase. *Curr. Biol.* **18,** 1649–1658
57. Vizcaíno, J. A., Côté, R., Reisinger, F., Foster, J. M., Mueller, M., Rameseder, J., Hermjakob, H., and Martens, L. (2009) A guide to the Proteomics Identifications Database proteomics data repository. *Proteomics* **9,** 4276–4283